Behavior and Design of High-Strength RC Walls

by J.W. Wallace

Synopsis: Use of high-strength reinforced concrete walls in regions of high seismic risk is evaluated using current U.S. code provisions, an example building, parametric studies, and experimental results. The format of current U.S. code provisions for structural walls promotes the use of high-strength concrete; however, the use of these provisions has not been evaluated for high-strength concrete. Analytical studies of building systems utilizing slender walls indicate that there is not a significant advantage associated with the use of high-strength concrete walls and that this advantage tends to diminish with increasing concrete strength. Evaluation of test results conducted in Japan for low-aspect ratio walls indicates that ACI 318-95 requirements do not represent the observed shear strength well. Based on the limited database considered in this study, a value of $1.0\sqrt{f_c'}$ MPa $\left(12\sqrt{f_c'}\text{ psi}\right)$ was found to provide a good estimate of wall shear strength.

Keywords: Earthquake-resistant structures; high-strength concrete; reinforced concrete; shear properties; strength; walls

John W. Wallace is an Associate Professor of Civil Engineering at the University of California, Los Angeles. His research and teaching interests include analysis, design, and experimental evaluation of reinforced concrete structural systems and elements. He is a member of ACI Committees 318-H, 352, 368, 369, and 442, and currently serves as the Chair of Committee 368.

INTRODUCTION

The use of reinforced concrete structural walls, or shear walls, to resist lateral loads is common in the United States (Eberhard and Meigs, 1995). Structural engineers cite the excellent performance of structural wall buildings in earthquakes as well as simplicity of design as primary reasons for using shear walls. In addition, stairwells and elevator cores provide the opportunity to use shear walls without adversely affecting the aesthetics or function of the building. The extensive use of shear walls has led to intensive scrutiny of design provisions used to proportion and detail shear walls (Wallace, 1996).

Current ACI code provisions for design of shears walls (*Building, 1995)* have been used without significant revision since the adoption of the 1983 Code (*Building, 1983).* The lateral and gravity forces exerted on the wall are assumed to be resisted by a tension-compression couple at the boundary regions assuming the wall web does not contribute significantly to wall flexural strength. Requirements for transverse reinforcement at the wall boundaries are assessed based on linear elastic models with a limiting extreme fiber compressive stress of $0.2f_c^{'}$. If the computed stress level is greater than $0.2f_c^{'}$, then well detailed boundary regions are required. This approach is relatively simple and is generally quite conservative with respect to required transverse reinforcement at wall boundaries (Wallace and Moehle, 1992). Given the format of the existing ACI provisions, there has been a tendency for designers to use higher strength concrete to avoid the need to provide well detailed regions at wall boundaries; however, this trend raises concern given the perceived brittleness of high-strength concrete. ACI 318-95 requirements for wall shear strength are also a function of the concrete compressive strength; therefore, there appear to be benefits associated with the use of high-strength concrete for walls controlled by shear. Little research has been conducted on the use of high strength concrete materials in regions of high seismic risk; therefore, no guidelines or significant reference materials exist that the designer can use to address behavior and design of walls constructed with high-strength concrete.

OBJECTIVES

Given the lack of research and reference materials on the use of high-strength concrete in regions of high seismic risk and the format of current ACI code provisions, a comprehensive review of behavior and design of shear walls constructed using high-strength concrete is needed. The review should include an evaluation of current design provisions as well as provide techniques that could be used by designers to accurately assess the benefits and limitations of using high-strength RC walls. These needs provide the basis for the topics addressed within this paper.

STRUCTURAL WALLS: CODE TRENDS

The prescriptive provisions of the current ACI building code *(Building, 1995)* as well as the conservative nature of provisions used in other countries (e.g., "Concrete," 1995; and "Eurocode 8," 1993) have received considerable attention within the United States in recent years. The primary motivation in this work has been the need to develop a "tool box" for the designer to assist in understanding expected wall behavior for either new or existing construction, as well as the potential applications of new materials. In this regard, it is clear that displacement-based design concepts (Moehle and Wallace, 1989; Wallace and Moehle, 1992) have gained widespread acceptance. Displacement-based design provides a flexible design and evaluation tool that can be incorporated relatively easily into design office practice, yet provides the engineer with broad information from which to assess wall behavior and expected performance. For these reasons, displacement-based design has been incorporated into the Uniform Building Code *(Uniform, 1994)* to evaluate detailing requirements at wall boundaries, and similar efforts are underway within ACI 318. In the following sections, behavior of structural walls is reviewed and design issues are discussed.

Displacement-Based Design of Structural Walls

To highlight the important steps involved in displacement-based design, consider the example building shown in Fig. 1. The building is 100 ft (30.48 m) by 75 ft (22.86 m) in plan and five stories tall. The story height is 12 ft (3.65 m) and the floor dead (including tributary wall, column, and partition weight) and live loads are 150 psf (7.18 kPa) and 40 psf (2.39 kPa), respectively. For purposes of

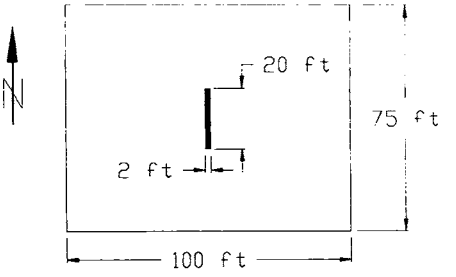

Fig. 1—Example building floor plan (1 ft = 0.0305m)

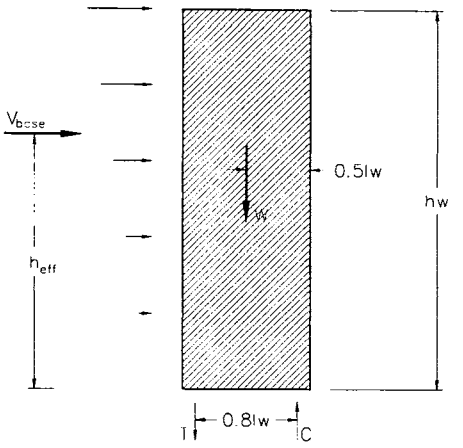

Fig. 2—Model to estimate wall longitudinal reinforcement

this discussion, only loads in the north-south direction are to be considered; therefore, a single wall is used to provide lateral force resistance in this direction. The wall dimensions are initially selected to be 20 ft (6.10 m) long by 2 ft (0.61 m) wide. The resulting wall aspect ratio is three and the ratio of wall area to total floor plan area is 0.0053.

Based on UBC (*Uniform, 1994*) requirements for a building located in Zone 4 (Z=0.4, S=1. I=1, T=0.43 sec, C=2.195, R_w=8), the unfactored base shear is 0.11W, where W=5,625 kips (25 MN) for a seismic dead weight of 150 psf (7.18 kPa); therefore, the unfactored base shear is 620 kips (2.76 MN). The distribution of the lateral force over the height of the building increases linearly with values of 40, 85, 125, 165, and 205 kips at the first through fifth levels, respectively (4448 N/kip).

UBC-94 load cases are used to assess flexural strength requirements. Assuming the wall resists the entire base shear force to simplify the analysis, the unfactored moment at the base of the wall is M = (205^kx60')+(165^kx48')+(125^kx36')+(85^kx24') + (40^kx 12') = 27,240 ft-kips (3.69 MN-m) and the effective height h_{eff} of the resulting lateral load is 27,240/620 = 44 ft (0.73h_w). Wall reinforcement at the base should be selected to resist this moment in combination with gravity loads for appropriate load combinations. A simplified model is used to estimate required wall boundary longitudinal reinforcement (Fig. 2) which assumes a moment arm of 0.8(20 ft) = 16 ft (4.88 m) between the tension and compression resultant in the wall and a tributary area of 1000 ft^2 (92.9 m^2)at each floor level (unfactored dead load of 750 kips (3.34 MN) at the centerline of the wall). Selection of tension reinforcement at the wall boundary is controlled by the following UBC-94 load case: 0.9DL ± 1.4EQ; therefore, the tension force at the wall boundary region is T = (1.4*27,240 ft-kips - 0.9*750 kips*8 ft)/16 ft = 2,045 kips (9.1 MN). The required area of tension steel is: A_s = 2,045 kips/60 ksi = 34 in^2 (21,935 mm^2). For this example, 14-#14 bars are provided (A_b = 2.25 in^2; 1,452 mm^2).

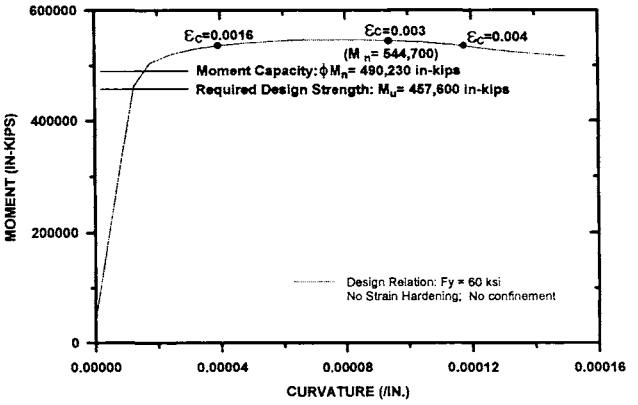

Fig. 3—Design moment-curvature relation

Because this evaluation is approximate, the design strength is verified using a moment-curvature analysis. Uniform web vertical reinforcement consists of two curtains of US #6 (A_b = 0.44 in^2; 285 mm^2) bars spaced at 12 inches (0.305 m) on center (ρ=0.003). The design moment-curvature relation, for US Grade 60 steel (f_y = 60 ksi; 413.7 MPa) neglecting the effects of strain hardening) and a concrete strength of 5 ksi (34.5 MPa), is plotted in Fig. 3. At an extreme fiber compression strain of 0.003, which is selected to be consistent with ACI 318-95 S10.2.3, the nominal moment capacity M_n is 544,700 in-kips (61.5 MN-m) and ϕM_n is 490,230 in-kips (55.4 MN-m), Since $\phi M_n \geq$ (M_u = 1.4*27,240 ft-kips = 457,620 in-kips; 51.7 MN-m), the wall flexural strength is adequate. It will be shown later in this paper that the maximum extreme fiber compression strain is less than 0.003 for the earthquake demands placed on the wall (Fig. 6); however, the flexural strength does not vary significantly for a fairly broad range of maximum compression strain for typical walls (from 0.0016 to 0.004, Fig. 3, for this example). At this stage of the evaluation, flexural strength may be evaluated for an extreme fiber compression strain of 0.003 subject to verification later in the evaluation process.

Figure 3 also illustrates the major disadvantage of using a stress-based approach to evaluate detailing requirements at wall boundaries. For a broad range of extreme fiber compression strains, approximately 0.001 to 0.006 for this example, the moment does not vary significantly. Therefore, a stress-based index such as used in ACI 318-95, which cannot assess the strain levels, has limited value.

Well established techniques can be used to assess the wall deformations required to achieve the displacement response the wall is expected to undergo. Consider the wall system shown in Fig. 4. The displacement at the roof level can be computed as:

$$\delta_{total,\,roof} = \delta_{elastic} + \delta_{inelastic} = \delta_y + \theta_p(h_w - l_p/2) \quad (1)$$

Where, $\delta_{elastic}$ and $\delta_{inelastic}$ are the elastic and inelastic components of the wall (roof) displacement, respectively. Since walls in reasonably-configured buildings will experience yielding (Wallace and Moehle, 1992), the elastic component of displacement response may be taken as δ_y, where δ_y is the roof displacement at first yield of wall boundary reinforcement. The inelastic component of displacement response can be computed by lumping the inelastic curvature over an assumed plastic hinge length l_p at the base of the wall. *Note that this model is only valid if steps are taken to ensure that significant inelastic deformations do not occur at levels other than at the base.* The length of the plastic hinge is selected such that the area under the actual curvature diagram is approximately equal to that for constant curvature over the plastic hinge length. Based on this model, the displacement at the top of the wall due to inelastic deformations is equal to the plastic hinge rotation θ_p (ϕ_u x l_p) times the distance from the centroid of the plastic hinge to the top of the wall.

Based on a linearly increasing distribution of lateral forces over the wall height, the displacement at the top of the wall at yield is:

$$\delta_y = \frac{11}{40} \phi_y h_w^2 \tag{2}$$

where, ϕ_y is the curvature at first yield of the wall boundary tension reinforcement. For walls with axial load of approximately 0.05 to $0.15A_g f_c'$, the curvature at the base of the wall at yield can be approximated as $0.0025/l_w$ to $0.0035/l_w$ (assuming that the tension reinforcement is US Grade 60 and has yielded, and that the extreme fiber concrete compression strain is between 0.0005 and 0.0015, see Wallace and Moehle, 1992). In general, it is wise to use a lower-bound estimate of yield curvature ($0.0025/l_w$) since this results in a low estimate for the wall yield displacement, and thus, requires greater inelastic deformations of the wall.

The displacement at the top of the wall due to inelastic deformations can be

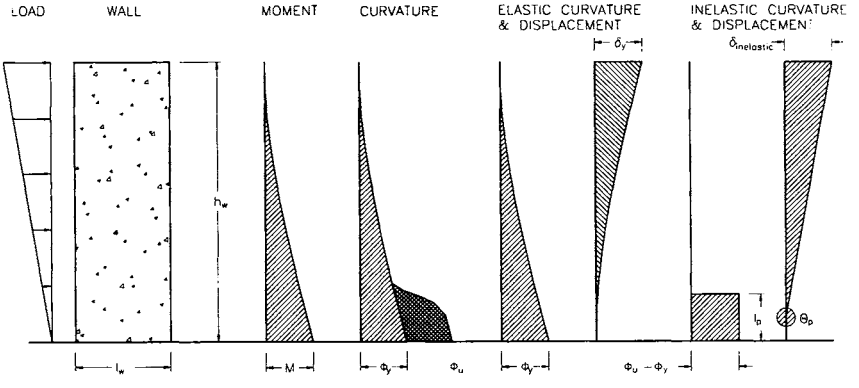

Fig. 4—Wall modeling and deformation components

computed as:

$$\delta_{inelastic} = \theta_p(h_w - l_p/2) = \left[(\phi_u - \phi_y)l_p\right](h_w - l_p/2) \quad (3)$$

where ϕ_u = the ultimate curvature developed at the base of the wall. A plastic hinge length of $0.5l_w$ is generally a good estimate for structural walls (Wallace and Moehle, 1992).

Based on these models, the ultimate curvature at the base of the wall can be computed given an estimated displacement response of the building. This topic is not addressed within this paper; the reader is referred to the following papers and reports (Wallace, 1996; Guidelines, 1995). For purposes of this discussion, a roof displacement of 5.75 inches (146 mm) is assumed. Using an estimate of the wall yield curvature of $0.0025/l_w$, the yield displacement is estimated as 1.5 inches (38 mm). Therefore, the inelastic wall deformations must account for a displacement of (5.75 - 1.5) = 4.25 inches (108 mm).

$$\delta_{inelastic} = (\phi_u - \phi_y)l_p(h_w - l_p/2) = (\phi_u - 0.0025/l_w)(0.5l_w)(h_w - 0.25l_w) = 4.25" \quad (4)$$

For a wall length of 20ft (240 inches; 6.1 m) and a wall height of 60ft (720 inches; 18.29 m), the ultimate curvature ϕ_u at the base of the wall is 0.0000643/inch (2.53E-6/mm). The ratio of the ultimate curvature to the yield curvature ($0.0025/l_w$ = 0.0000104/in.= 0.409E-6/mm), or the curvature ductility μ_ϕ, is 6.2, which is relatively low; therefore, transverse reinforcement at the wall boundaries is more likely to be controlled by buckling requirements than by confinement requirements. In general, an iterative approach must be used where the required transverse reinforcement is estimated and then verified by using a moment-curvature analysis (Wallace, 1995). This topic is addressed in the following paragraphs (also see Fig. 6 and 7).

Requirements for concrete confinement can be assessed by using a moment-curvature analysis. Recent experimental studies (Taylor, Thomsen and Wallace, 1996) indicate that moment-curvature response reasonably predicts flexural strength, stiffness and curvature capacity of slender structural walls. Realistic models for both reinforcement and concrete should be used in this analysis. For reinforcement, the effects of steel over-strength and strain hardening should be included when assessing detailing requirements since both of these parameters tend to be detrimental to wall deformation capacity. The confined concrete model proposed by Saatcioglu and Razvi (1992) was used in this study. The model accounts for the size, spacing, and distribution of transverse reinforcement as well as the distribution of longitudinal reinforcement.

Assuming that moderate-level details as shown in Fig. 5 are appropriate for this wall, the moment-curvature relation was computed and is plotted in Fig. 6. For comparison, two relations are plotted in Fig. 6. One curve (probable) includes the influence of steel over-strength, steel strain hardening, and concrete confinement using the Saatcioglu and Razvi model; the second curve (design) does not include these factors.

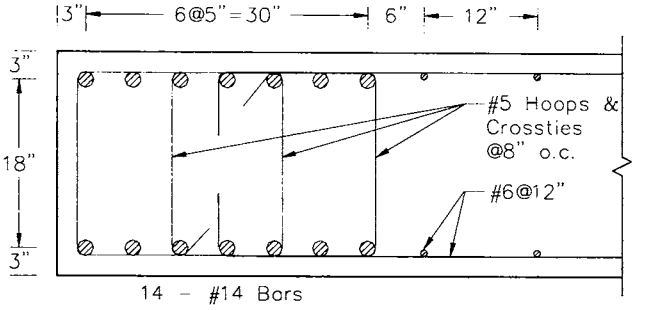

Fig. 5—Wall boundary reinforcement at base of wall
1 in. = 25.4 mm

The results plotted in Fig. 6 indicate that the wall has sufficient curvature capacity to meet the curvature demand from the design earthquake. In fact, the plots indicate that confinement is not required to meet the deformation demands imposed by the earthquake. The maximum concrete compressive strain at the extreme fiber is approximately 0.0026 for the relation based on probable wall moment-curvature response; therefore, for this relatively low compression strain, transverse reinforcement at the wall boundary is controlled by bar buckling versus concrete confinement. A spacing of $8d_b$ is adequate to control buckling (Wallace, 1995).

It is interesting to consider what current ACI requirements would dictate for this wall design. For combined lateral and gravity loads, the following load case is used to evaluate design requirements: 0.75(1.4DL + 1.7LL ± 1.1*1.7E). The unfactored dead and live loads are 750 kips and 200 kips, respectively, and the unfactored moment from the lateral load analysis is 27,240 ft-kips. An extreme fiber compression stress of P/A + M/S = 1042 kips/(240 x 24) in^2 + (6)[38,136(12) in.-kips]/(24 x 240^2) in^3 = 0.18 + 1.99 = 2.17 ksi (15 MPa) is computed. For 5 ksi concrete (34.5 MPa), a limiting stress of $0.2f_c'$ = 1.0 ksi (6.9 MPa) is computed; therefore, well detailed boundary elements are required according to ACI 318-95 requirements. A concrete strength of 2.17/0.2 = 10.85 ksi (74.8 MPa) is required to eliminate the need to provide the well-detailed boundary elements. However, the displacement-based evaluation indicates that relatively low compressive strains are expected, and thus, increasing the concrete strength is not necessary. ACI 318 requirements indirectly promote the use of high-strength concrete by using a stress-based index; however, the actual behavior of HSC walls must be considered to assess the potential benefits or drawbacks.

Behavior of the wall constructed with 12 ksi (82.7 MPa) concrete is evaluated using a moment-curvature analysis. Results are plotted in Fig. 7 for walls with 5 (34.5) and 12 ksi (82.7 MPa) concrete using the models proposed by Razvi for moderate and high-strength concrete (Razvi, 1995). Although the influence of confinement is included in the analysis, it has almost no effect over the range of the results plotted due to the relatively low compressive strain levels. The results indicate that the wall constructed with high-

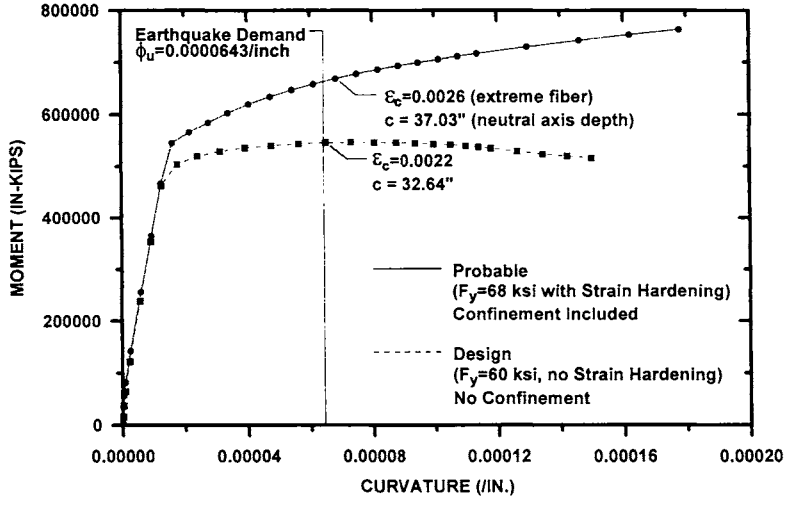

Fig. 6—Moment curvature relations. 1 in. = 25.4 mm; 1 ksi = 6.895 MPa; 1 kip = 4448 N

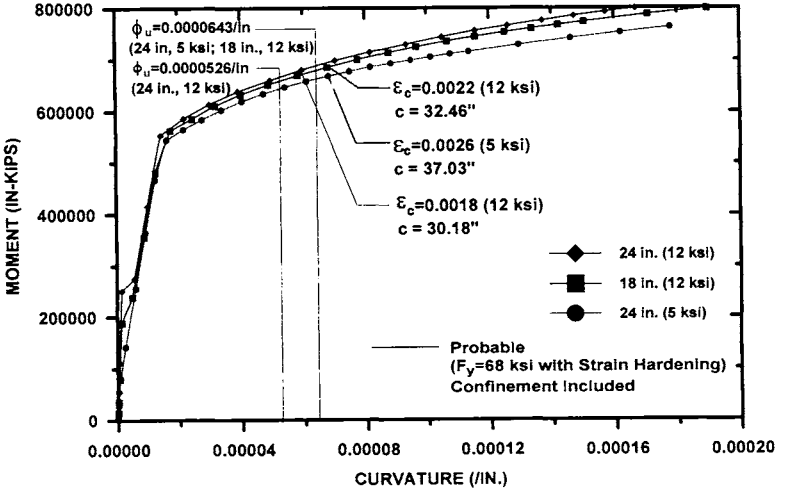

Fig. 7—Moment curvature response: influence of concrete strength. 1 in. = 25.4 mm; 1 ksi = 6.895 MPa; 1 kip = 4448 N

strength concrete is slightly stiffer (due to the higher modulus of 5,400 ksi (37,235 MPa) for the 12 ksi (82.7 MPa) concrete compared with a modulus of 3,800 ksi (26,200 MPa) computed using the relation proposed by ACI Committee 363 (1984)) and possesses slightly greater flexural strength (due to the shallower compression zone increasing the moment arm between the tension-compression couple). Ultimate curvature demand for the wall constructed with 12 ksi (82.7 MPa) concrete is less than that for the 5 ksi (34.5 MPa) wall and is estimated based on a roof displacement of $\sqrt{E_{c,5\ ksi} / E_{c,12\ ksi}}$ (5.75 in.) = 4.82 inches (122.4 mm). Figure 7 indicates that there may be a slight advantage to using high-strength concrete; however, it should be noted that identical cross-sections were used for the comparison. One of the advantages generally associated with the use of HSC is the use of smaller cross sections. For this example, the length of the wall (240 in.; 6.1 m) would not likely be changed; however, the wall thickness could be reduced (e.g., to 18 inches; 457.2 mm) and not affect the placement of the reinforcement (this would not likely be the case for a majority of wall cross sections). The reduced flexural stiffness associated with the reduced wall thickness would increase the ultimate curvature demand to slightly greater than that for the 5 ksi wall (34.5 MPa). The moment-curvature response for the 18 in. (457.2 mm) thick wall (Fig. 7) indicates that the advantages of using HSC for slender walls is not significant since the reduction in wall thickness is marginal and deformation demands are not reduced, and may actually increase. As well, the performance benefits associated with using the thicker wall (24 in.; 609.6 mm)) are relatively minor. The increased cost associated with the use of HSC is likely to more than offset these benefits.

Although the results presented in the preceding discussion are likely to be quite general, they revolve around a single example. Parametric studies are presented in the following section so that more general conclusions can be reached.

Generalized Analytical Studies of Slender HSC Walls

Displacement-based design of RC structural walls can be generalized using the procedures presented by Wallace (1994). The procedure allows for the direct evaluation of maximum compressive strain levels anticipated for a given building utilizing walls as the primary earthquake resisting structural system. The parametric studies are based on combining estimates of displacement response using single-degree-of-freedom models with equilibrium requirements for the wall cross section. The period estimate is based on the equation proposed by Sozen (1989) (see Wallace and Moehle, 1992):

$$T_{cracked} = 8.8 \frac{h_w}{l_w} n \sqrt{\frac{wh_s}{gE_c p}} \tag{5}$$

where n is the number of stories, w is the unit floor weight including tributary

wall weight, h_s is the mean story height, E_c is the concrete modulus of elasticity, h_w is the wall height, and p is the ratio of wall web area to floor plan area for the walls aligned in the direction the period is being calculated. The roof displacement response δ_u is calculated as:

$$\delta_u = 1.5\, S_d = 1.5\,(6T_{cracked}) \text{ inches} = 1.5\,(150T_{cracked}) \text{ mm} \qquad (6)$$

where S_d is the spectral displacement for a single-degree-of-freedom system. The ultimate curvature demand ϕ_u is calculated as (Wallace and Moehle, 1992):

$$\phi_u = 0.0025\left[1 - \frac{1}{2}\frac{h_w}{l_w}\right] + 2\frac{\delta_u}{h_w} \qquad (7)$$

Therefore, the ultimate curvature imposed on a wall cross section is directly related to the wall aspect ratio and the roof drift ratio (note that an assumed curvature at first yield of $0.0025/l_w$) is assumed in (7)). The extreme fiber compression strain can be computed directly from equilibrium requirements (Wallace 1994). For the evaluation of moderate-strength concrete walls, a Whitney Stress Block is used, whereas the equivalent stress block proposed by Park and Tanaka (1997) is used to model the stress block for high-strength walls. Based on these models, the following equation is derived for computing extreme fiber compression strain:

$$\varepsilon_{cu} = \left[\frac{\left(\rho + \rho'' - \frac{\gamma}{\alpha}\rho'\right)\frac{\alpha f_y}{f_c'} + \frac{P}{l_w t_w f_c'}}{\left(\alpha_1\beta_1 + 2\rho''\frac{\alpha f_y}{f_c'}\right)}\right]\phi_u l_w \qquad (8)$$

where ε_{cu} is the extreme fiber compression strain, $\rho = A_s/t_w l_w$ is the tension steel reinforcing ratio, $\rho' = A'_s/t_w l_w$ is the compression steel reinforcing ratio, $\rho'' = A''_s/t_w l_w$ is the distributed web steel reinforcing ratio, β_1 and α_1 are factors to define the depth and stress intensity of the equivalent rectangular stress block as given by Park and Tanaka (1997), P is the axial load level at ultimate lateral displacement, f_y is the nominal yield stress of the longitudinal steel, t_w is the wall thickness, l_w is the wall length, and α and γ are factors to account for over-strength and strain hardening of tension and compression steel, respectively (values of 1.5 and 1.25 are assumed, respectively).

Results are presented in Fig. 9 for two analyses. Values of w of 175 psf (8.38 kPa) and h_s of 120 in. (3.05 m) are assumed for use in Eq. (5). The first analysis (Fig. 9a), compares the computed extreme fiber strain for rectangular walls with identical cross sections for concrete strengths of 4, 8, and 12 ksi (27.6, 55.2, and 82.7 MPa). Axial load is varied in proportion to the concrete strength with a reference value of $0.10A_g f_c'$ for the wall with 4

ksi concrete. The results indicate that there is a distinct advantage in using high-strength concrete walls in this case, although the advantage is diminished for concrete strengths greater than 8 ksi (55.2 MPa). The lower strain levels result from the stiffer wall reducing lateral drift relative to the 4 ksi (27.6 MPa) concrete wall and also because of the shorter depth of the compression zone for the higher strength concrete. For the second analysis (Fig. 9b), also for walls with 4, 8 and 12 ksi concrete (27.6, 55.2, and 82.7 MPa), the wall axial load is held constant by decreasing the wall thickness for the walls constructed of higher-strength concrete; therefore, the ratio of wall thickness is: 1(4 ksi):0.5 (8 ksi):0.33(12 ksi). The depth of the compression zone is nearly equal for all three cases plotted in Fig. 9(b); therefore, the increase in strain observed for the higher strength concrete is a result of the reduction in the flexural stiffness EI (E increases less than I decreases), such that lateral drift increases. It is noted that cover and spacing requirements for the reinforcement (particularly at splices) may dictate a minimum wall thickness. Use of reinforcement with higher yield stress may prove useful in reducing wall thickness.

In general, special transverse reinforcement for concrete confinement and for restraint of longitudinal bar buckling is used where compression strains exceed 0.003 *(Uniform, 1994)* for walls constructed of moderate-strength concrete. A similar requirement could be used for high-strength concrete; however, given the uncertainty in predicted displacement response of buildings, greater conservatism may be prudent for HSC walls, even for strain levels below 0.003, to accommodate the relatively brittle behavior of "unconfined" HSC. As well, it should be noted that greater quantities of transverse reinforcement are needed to confine high-strength concrete (ACI Committee 363, 1984); therefore, there may be additional costs associated with the use of high-strength concrete.

The analysis results clearly indicate that there are no significant advantages associated with the use of high-strength concrete for slender structural walls. Use of concrete strengths up to 8 ksi (55.2 MPa) may provide marginal advantages; however, careful consideration of the affects of changing the concrete strength on overall response and behavior of the structural system must be considered. These factors are easily evaluated in a displacement-based design format.

Evaluation of Low Aspect Ratio Walls

Design requirements for low aspect ratio walls are typically based on comparing an average shear stress with a nominal shear stress capacity. According to ACI 318-95 requirements, the nominal wall shear strength is computed as:

$$V_n = A_{cv}\left(\alpha_c \sqrt{f_c'} + \rho_n f_y\right) \tag{9}$$

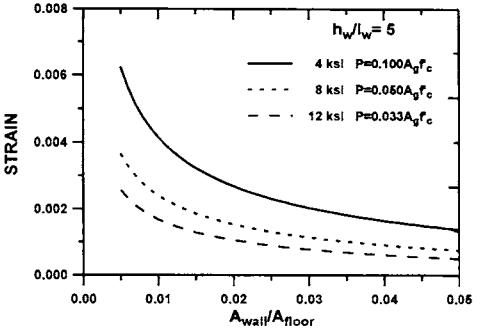

Fig. 9A—Extreme fiber compression strain for walls with constant cross section

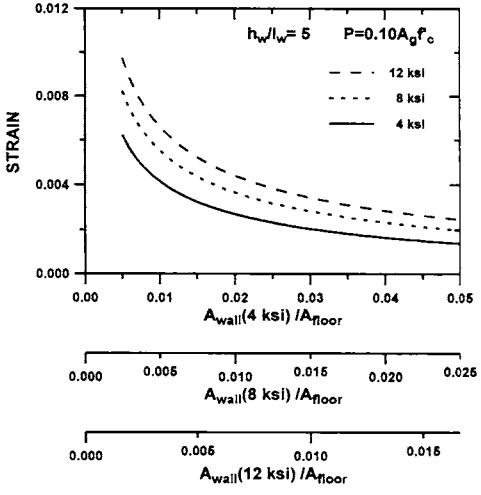

Fig. 9B—Extreme fiber compression strain for walls with constant level of axial stress

where A_{cv} is the area bounded by the web thickness and the wall length, α_c is a coefficient that varies from 3.0 for h_w/l_w = 1.5 to 2.0 for h_w/l_w = 2.0, and ρ_n is the ratio of distributed shear reinforcement perpendicular to the plane A_{cv}. The wall shear strength is limited to a maximum value of $10A_{cv}\sqrt{f'_c\ psi}$ $\left(0.83A_{cv}\sqrt{f'_c\ MPa}\right)$ for an individual wall and $8A_{cv}\sqrt{f'_c\ psi}$ $\left(0.67A_{cv}\sqrt{f'_c\ MPa}\right)$ for all walls providing lateral load resistance. For design, $\phi V_n \geq V_u$, where V_u is computed as the wall shear force determined from appropriate load combinations for the given loads.

Research conducted and reviewed by Aktan and Bertero (1985) suggests that the ACI provisions are unconservative; therefore, they recommend a limit on wall shear stress of $6\sqrt{f'_c\ psi}$ $\left(0.5\sqrt{f'_c\ MPa}\right)$. Wood (1990) also reviewed ACI provisions, as well as simplified models for shear strength using an extensive database of test results. Based on this review, the following equation was proposed to provide a lower bound estimate of wall shear strength:

$$V_n = \text{the larger of } \left\{A_{cv}6\sqrt{f'_c\ psi};\ A_{vf}f_y/4\right\} \leq A_{cv}10\sqrt{f'_c\ psi} \quad (10a)$$

$$V_n = \text{the larger of } \left\{A_{cv}0.5\sqrt{f'_c\ \text{MPa}};\ A_{vf}f_y/4\right\} \leq A_{cv}0.833\sqrt{f'_c\ \text{MPa}} \quad (10b)$$

where A_{vf} is the total area of vertical reinforcement. An alternative approach, based on a combined arch and truss mechanism, is presented by Kabeyasawa and Hiraishi (1996) and appears to give reliable results for wall tests conducted in Japan.

Experimental Results for HSC Low Aspect Ratio Walls

Experimental results for low aspect ratio walls constructed with high-strength concrete are scarce. The majority of tests have been conducted in Japan by Kabeyasawa et al (1993; 1994; 1997). These tests are presented and discussed in detail in a related paper within this special publication; therefore, the focus of this discussion is on the review of code expressions used within the United States. Specimen labels as well as an identification number for the plots that appear later in this paper are listed in Table 1, column 1. The maximum shear observed during the test is given in Table 1, column 2.

To evaluate whether flexural or shear type failures were expected for the wall specimens, the shear at flexural capacity was computed using the approximate relationship used in Japan to allow for direct comparison of results presented by Kabeyasawa and Hiraishi (1997):

$$M_n = A_t f_y l_w + 0.5 A_w f_{wy} l_w + 0.5 P l_w \tag{12}$$

where M_n is the nominal flexural capacity, A_t and f_y are the area and yield stress of longitudinal boundary reinforcement, A_w and f_{wy} are the area and yield stress of the vertical web reinforcement, and P is the axial load. The ratio of the maximum shear measured during the test to the shear at flexural capacity is listed in Table 1, column 3. Based on these ratios, "shear" failures are expected for all walls (except NW-1) prior to reaching the flexural capacity of the walls; therefore, it is appropriate to evaluate wall shear strength expressions using the entire database. For several walls (NW-1, W8N13, and W8N8H), flexural capacity is likely to be reached given the expressions for shear strength tend to give a conservative (Eq. 9) or lower bound (Eq. 10) estimate of wall shear strength.

Ratios of the measured maximum shear V_{max} to the computed strength V_n using equations (9) and (10) are listed in Table 1 (columns 5 and 6). Measured shear strengths are 1.38 times the shear strength obtained using the ACI 318-95 equation. The greatest discrepancies exist for lightly reinforced sections (e.g., specimens NO. 1 and NO. 2, ID's 9 and 10). Shear strength ratios for the ACI 318-95 equation are plotted versus $\rho_n f_y / f_c^{'}$ in Fig. 10. The plot reveals that the ACI equation underestimates the shear strength at low ratios of $\rho_n f_y / f_c^{'}$ and overestimates shear strength at higher ratios.

TABLE 1—HSC WALL TESTS CONDUCTED IN JAPAN

Specimen ID	V_{max} (kN)	$\frac{V_{max}}{V_u@M_n}$	$\frac{V_n\ Eq.(9)}{V_u@M_n}$	$\frac{V_{max}}{V_nEq(9)}$	$\frac{V_{max}}{V_nEq(10)}$	$\frac{V_{max}}{\sqrt{f_c'\ MPa}}$	$\frac{\rho_n f_y}{f_c'}$	$\frac{A_{vf} f_y}{A_{cv} f_c'}$	$\frac{\rho_t f_{yt}}{f_c'}$
(1)	(2)	(3)	(4)	(5)	(6)	(7)	(8)	(9)	(10)
NW-1 (1)	1062	1.03	0.91	1.13	1.67	0.83	0.061	0.16	0.23
NW-2 (2)	1468	0.95	0.61	1.55	2.23	1.12	0.057	0.15	0.21
NW-3 (3)	717	0.84	0.52	1.62	1.42	0.71	0.036	0.22	0.24
NW-4 (4)	784	0.75	0.42	1.78	1.48	0.78	0.037	0.29	0.25
NW-5 (5)	900	0.86	0.69	1.25	1.54	0.85	0.067	0.29	0.22
NW-6 (6)	1056	0.86	0.59	1.45	1.52	0.96	0.062	0.31	0.21
W-08 (7)	1670	0.35	0.24	1.48	2.42	1.21	0.056	0.14	0.24
W-12 (8)	1719	0.32	0.22	1.46	2.16	1.08	0.042	0.10	0.18
NO. 1 (9)	1101	0.30	0.13	2.25	1.21	1.00	0.024	0.48	0.31
NO. 2 (10)	1255	0.33	0.17	1.90	1.32	1.10	0.039	0.46	0.28
NO. 3 (11)	1379	0.35	0.22	1.60	1.44	1.20	0.059	0.47	0.31
NO. 4 (12)	1697	0.37	0.20	1.84	1.50	1.23	0.041	0.32	0.22
NO. 5 (13)	1159	0.45	0.30	1.50	1.17	0.97	0.055	0.44	0.29
NO. 6 (14)	1412	0.33	0.23	1.45	1.45	1.21	0.126	0.50	0.30
NO. 7 (15)	1499	0.36	0.23	1.57	1.57	1.30	0.111	0.51	0.31
NO. 8 (16)	1639	0.37	0.23	1.66	1.66	1.38	0.151	0.51	0.29
M35X (17)	1049	0.63	0.54	1.17	1.95	0.98	0.104	0.25	0.15
M35H (18)	1055	0.61	0.55	1.12	1.87	0.94	0.094	0.23	0.14
P35H (19)	959	0.57	0.55	1.04	1.73	0.87	0.097	0.24	0.07
M30H (20)	1020	0.67	0.58	1.15	1.91	0.96	0.106	0.25	0.16
MW35H (21)	1012	0.63	0.54	1.16	1.91	0.96	0.109	0.26	0.16
MAE03 (22)	1460	0.27	0.19	1.46	2.19	1.10	0.066	0.25	
MAE07 (23)	1676	0.28	0.18	1.51	2.31	1.26	0.110	0.29	
W48M6 (24)	1516	0.57	0.52	1.10	1.62	0.81	0.054	0.10	
W48M4 (25)	1479	0.61	0.55	1.12	1.58	0.79	0.050	0.09	
W72M8 (26)	2066	0.57	0.43	1.33	2.21	1.10	0.088	0.16	
W72M6 (27)	2015	0.59	0.46	1.29	2.15	1.08	0.081	0.15	
W72M8 (28)	2128	0.59	0.48	1.23	2.04	1.02	0.071	0.13	
W96M8 (29)	2483	0.55	0.38	1.43	2.39	1.19	0.092	0.17	
SMZ01 (30)	1154	0.37	0.29	1.30	1.25	0.62	0.025	0.09	0.02
SMZ03 (31)	2081	0.33	0.14	2.35	2.25	1.13	0.025	0.18	0.02
W8N18 (32)	882	0.78	0.71	1.85	1.85	0.92	0.137	0.18	0.15
W8N13 (33)	762	0.80	0.87	1.53	1.53	0.77	0.126	0.17	0.14
W8N8H (34)	689	0.76	0.92	1.38	1.38	0.69	0.126	0.20	0.13
TAK01 (35)	971	0.59	0.62	1.52	1.52	0.76	0.077	0.17	0.10
TAK02 (36)	987	0.55	0.59	1.55	1.55	0.77	0.111	0.20	0.10
TAK03 (37)	1288	0.52	0.43	2.02	2.02	1.01	0.077	0.17	0.10

The ACI 318-95 equation does seem to properly differentiate between walls that approach their flexural strength and thus, may exhibit some flexural ductility prior to failure versus walls that fail in shear without reaching their flexural strength (e.g., see Table 1, columns 4 and 6, for specimens NW-1 through NW-6). The inability of the ACI equation to provide a more accurate prediction of shear capacity is likely a function of the rather crude format of the equation as well as the inability of the equation to account for the effects of boundary column confinement on web shear strength. Confined boundary columns would be expected to increase the web shear strength by providing

an effective confining pressure on the wall web (Bonacci, 1994). Therefore, for the specimens reviewed in this paper, all of which have fairly significant boundary column confinement, the ACI equation would be expected to underpredict shear strength. Measured shear strength normalized by the square root of the compressive strength is plotted versus the transverse reinforcing ratio times the yield strength of the transverse reinforcement normalized by the concrete strength in Figure 11. The plot reveals that measured shear strength does increase with the amount of confining pressure provided; however, given the scatter observed in the figure, the trend is not strong.

Results for the equation suggested by Wood (1990) are plotted in Fig. 12 and reveal that the expression gives relatively conservative results. This suggests that the lower bound estimate of shear strength of $0.5A_{cv}\sqrt{f_c'}$ MPa is not valid for HSC. This is not unexpected given the greater tensile capacity of high-strength concrete (ACI Committee 363, 1983). Figures 13 and 14 plot the ratio of the measured shear strength normalized to the square root of f_c' versus $\rho_n f_y / f_c'$ and $A_{vf} f_y / A_{cv} f_c'$, respectively. The average shear strength is $0.99A_{cv}\sqrt{f_c'}$ MPa with a standard deviation of $0.19A_{cv}\sqrt{f_c'}$ MPa. Figure 13 reveals that the web reinforcing ratio does not have a significant influence on wall shear strength and that a good lower bound estimate of the wall shear strength is $0.75A_{cv}\sqrt{f_c'}$ MPa. Figure 14 indicates that shear strength does increase for ratios of $A_{vf} f_y / A_{cv} f_c'$ greater than 0.4; however, the trend is not strong.

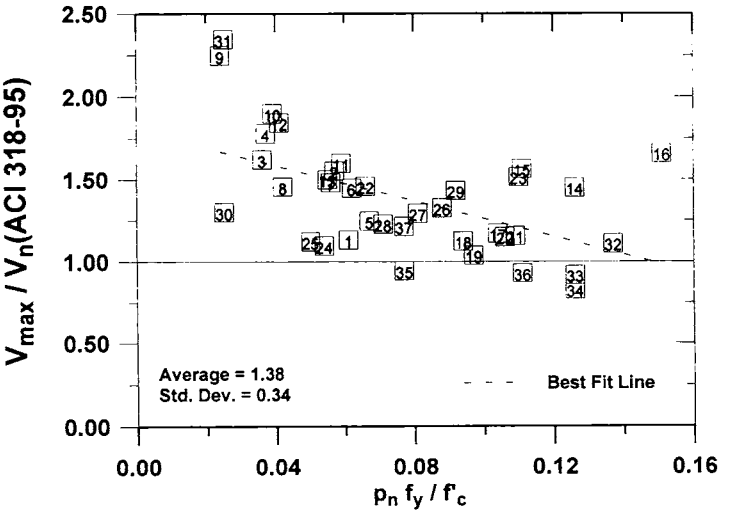

Fig. 10—Wall shear strength: ACI 318-95

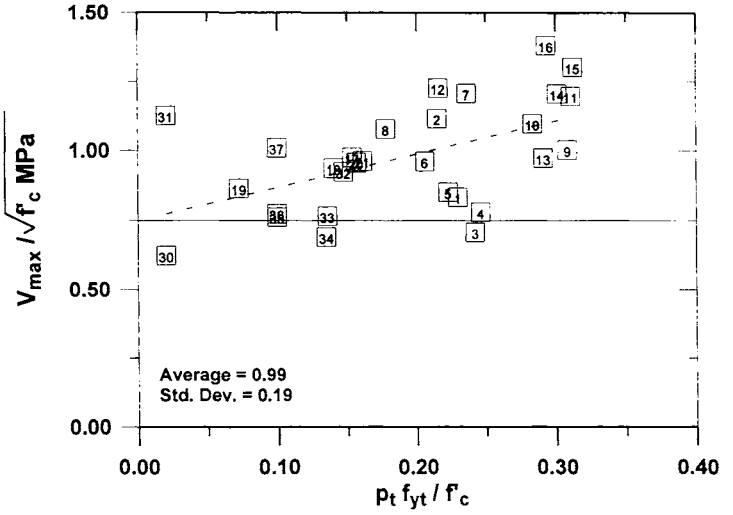

Fig. 11—Wall shear length—Influence of boundary confinement

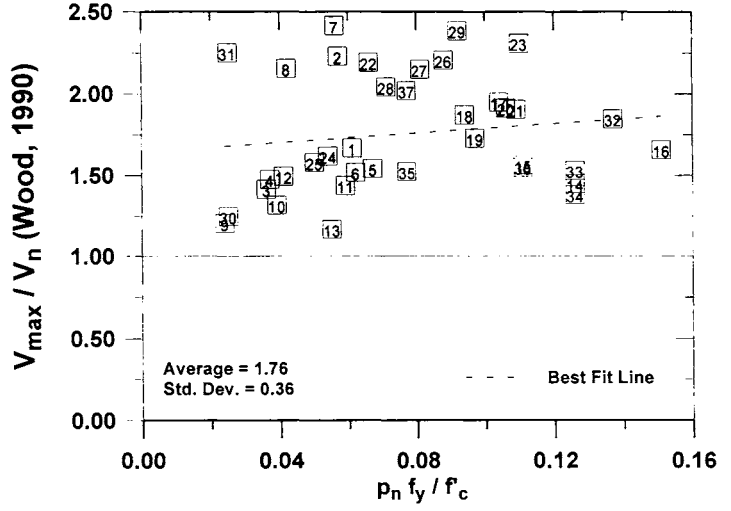

Fig. 12—Wall shear strength: Wood (1990)

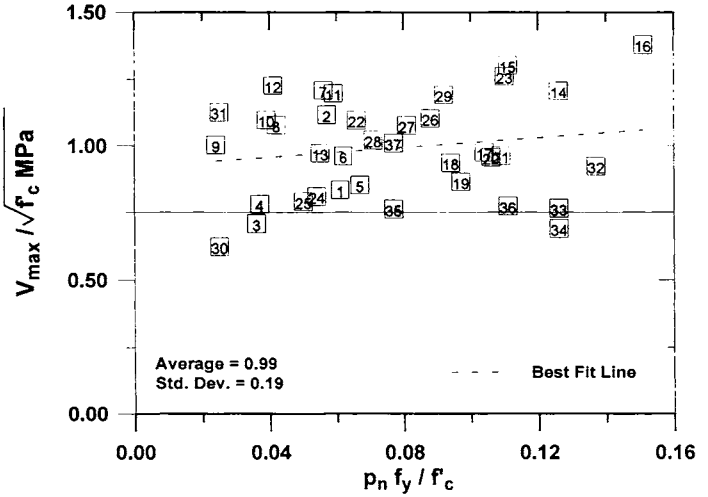

Fig. 13—Wall shear strength—Influence of web reinforcement

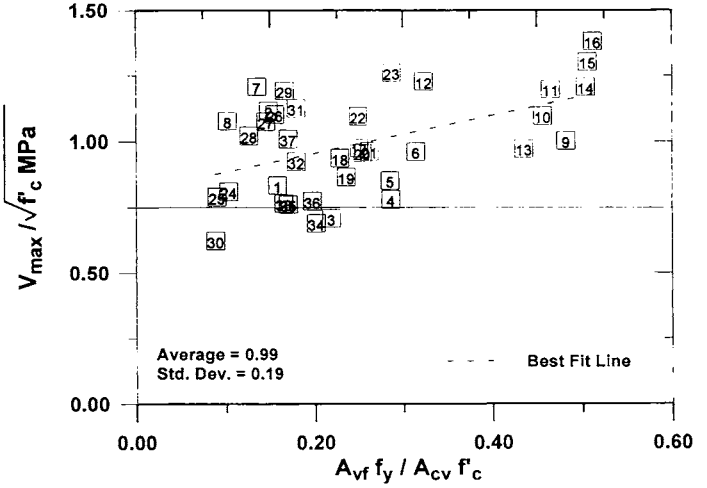

Fig. 14—Wall shear strength—Influence of vertical reinforcement

The test results reported by Kabeyasawa and Hiraishi (1996) indicate that a majority of wall "shear" failures for HSC walls were abrupt with little observed inelastic energy dissipation capacity. Therefore, design of HSC walls may require that the walls remain essentially elastic for the forces and deformations expected to occur in the design earthquake. Actual forces and deformations should be considered, and not code level forces and deformations reduced by R_w.

It should be noted that the database used in this evaluation is somewhat limited (37 specimens) and that there is not substantial variation in the specimen details. Therefore, the results show less scatter than those reported for moderate-strength concrete (for example, see Wood, 1990).

SUMMARY & CONCLUSIONS

Given the format of current U.S. design provisions for shear walls, use of high-strength concrete is likely to be seen to have significant advantages for both slender and squat walls. The objective of this paper was to review these code provisions and to systematically study wall behavior to establish the potential benefits and shortcomings of structural walls constructed of high-strength concrete.

For slender walls, there are benefits associated with the use of high-strength concrete; however, these benefits diminish significantly for concrete strengths greater than approximately 55 MPa (8 ksi). One of the primary benefits typically attributed to the use of high-strength concrete, the use of smaller cross sections, may actually lead to greater deformations on the wall since wall inertia tends to decrease at a faster rate than the modulus of elasticity increases. In addition, use of thinner walls may not be possible due to spacing requirements for longitudinal reinforcement. For these reasons, use of concrete strength greater than approximately 55 MPa (8 ksi) is not likely to be cost effective for slender walls.

Wall flexural strength should be evaluated using a modified equivalent rectangular stress block, such as that suggested by Park and Tanaka (1996). Relationships that have been verified for high-strength concrete, for example, the relationship proposed by Razvi (1995), should also be used to establish moment-curvature response.

A review of experimental work on low-aspect ratio walls conducted in Japan indicates that the expression used in ACI 318-95 to compute wall shear strength tends to give conservative results and overestimates the influence of the web reinforcing ratio on wall shear strength. For the 37 wall tests reviewed, the wall shear strength can be represented reasonably well as a multiple of the square root of the concrete compressive strength with an average shear strength of $1.0\sqrt{f_c' \text{ MPa}}$ $\left(12\sqrt{f_c' \text{ psi}}\right)$ and a standard deviation of $0.2\sqrt{f_c' \text{ MPa}}$ $\left(2.4\sqrt{f_c' \text{ psi}}\right)$. Due to the brittle failure modes reported for low-aspect ratio walls, behavior should be evaluated for forces and deformations expected to develop for the design earthquake.

REFERENCES

ACI Committee 363, "State of the Art Report on High-Strength Concrete," *Journal of the American Concrete Institute,* Vol. 81, No. 4, pp. 364-411, (July-August, 1984).

Aktan, A. E. and Bertero, V. V., "RC Structural Walls: Design for Shear," *Journal of Structural Engineering,* ASCE, Vol. 111, No. 8, pp. 1775-1791, (August 1985).

"Building Code Requirements for Structural Concrete (ACI 318-95) and Commentary (ACI-318R-95)," American Concrete Institute, Farmington Hills, MI, (1995).

"Building Code Requirements for Structural Concrete (ACI 318-83) and Commentary (ACI-318R-83)," American Concrete Institute, Farmington Hills, MI, (1983).

"Concrete Design Standard, NZS 3101:1995 Part 1 and Commentary on the Concrete Design Standard, NZS 3101:1995 Part 2," Standards Association of New Zealand (1995).

Eberhard, M. O. and Miegs, B. E., "Earthquake-Resisting System Selection for RC Buildings," *Earthquake Spectra,* Vol. 11, No. 1, pp. 19-36 (February 1995).

"Eurocode 8 - Earthquake-Resistant Design of Structures - General Rules and Rules for Buildings," Commission of the European Communities, Second Draft, (1993).

"Guidelines for the Seismic Rehabilitation of Buildings: 75% Compete Draft," Applied Technology Council, Redwood City, CA (December 1995).

Kabeyasawa, T., Kuramoto, H., and Matsumoto, K., "Tests and Analyses of High Strength Shear Walls, *Proceedings*, First Meeting of the Multilateral Project on the Use of High Strength Concrete, Kyoto, Japan, (May 1993).

Kabeyasawa, T., Hiraishi, H., and Kumagai., "Tests and Analyses of High Strength Shear Walls in Japan, *Proceedings*, Second US-Japan-New Zealand-Canada Multilateral Meeting on Structural Performance of High Strength Concrete in Seismic Regions, Honolulu, Hawaii, (December 1994).

Kabeyasawa, T., Hiraishi, H., "Tests and Analyses of High Strength Shear Walls in Japan, *ACI SP,* American Concrete Institute, Farmington Hills, MI (1997).

Moehle, J. P.; Wallace, J. W., "Ductility and Detailing Requirements of

Shear Wall Buildings," *Proceedings*, 5th Chilean Conference on Seismology and Earthquake Engineering, Santiago, Chile; 131-150, (August 1989).

Park, R. and Tanaka, H., "High Strength Concrete Columns," *Proceedings,* Second US-Japan-New Zealand-Canada Multilateral Meeting on Structural Performance of High Strength Concrete in Seismic Regions, Honolulu, Hawaii, (December 1994).

Park, R. and Tanaka, H., "High Strength Concrete Columns," *ACI SP,* American Concrete Institute, Farmington Hills, MI (1997).

Razvi, S. R., "Confinement of High-Strength Concrete Columns," *Ph.D. Thesis,* University of Ottawa, Ottawa, Ontario, Canada, (June 1995).

Saatcioglu, M. & Razvi, S. R., "Strength and Ductility of Confined Concrete," *Journal of Structural Engineering,* ASCE, Vol. 118, No. 6, pp. 1590-1607, (June 1992).

Taylor, C. P.; Thomsen IV, J. H.; and Wallace, J. W., "Experimental Verification of Displacement-Based Design Procedures for Slender RC Structural Walls," *Proceedings,* 11th World Conference on Earthquake Engineering, Acapulco, Mexico, (June 1996).

"Uniform Building Code", International Conference of Building Officials, Whittier, California, (1994).

Wallace, J. W., "A New Methodology for Seismic Design of RC Shear Walls," *Journal of Structural Engineering,* ASCE, Vol. 120(3): pp. 863-884, (March 1994).

Wallace, J. W., ``Evaluation of UBC-94 Provisions for Seismic Design of RC Structural Walls," *Earthquake Spectra,* Vol. 12, No. 2, (May 1996).

Wallace, J. W.; Moehle, J. P., "Ductility and Detailing Requirements of Bearing Wall Buildings," *Journal of Structural Engineering,* ASCE, Vol. 118(6): 1625-1644, (June 1992).

Wood, S. L., "Shear Strength of Low-Rise Reinforced Concrete Walls," *ACI Structural Journal,* 87(1): 99-107, (January-February 1990).